

and *Semimetals*, edited by R. K. Willardson and A. C. Beer (Academic, New York, 1966), Vol. 1, p. 159.

⁶F. Stern and W. E. Howard, *Phys. Rev.* **163**, 816 (1967).

⁷See, for example, *Proceedings of the International Conference on Electronic Properties of Quasi-Two-Dimensional Systems, Providence, Rhode Island, 1976*, edited by J. J. Quinn and P. J. Stiles (North-Holland,

Amsterdam, 1976) as reprinted from *Surface Science* **58**, 1976.

⁸T. Ando and Y. Uemura, *J. Phys. Soc. Jpn.* **36**, 959 (1974).

⁹F. F. Fang and P. J. Stiles, *Phys. Rev.* **174**, 823 (1968).

¹⁰M. H. Cohen and L. M. Falicov, *Phys. Rev. Lett.* **7**, 231 (1961).

Positron Self-Trapping in ⁴He

M. J. Stott* and E. Zaremba

Department of Physics, Queen's University, Kingston, Ontario, Canada K7L 3N6

(Received 7 April 1977)

Positron-annihilation experiments in helium gas have shown anomalies in annihilation rate near the gas-liquid critical point which indicate the formation of positron self-trapped states in helium droplets. We present theory which appears to confirm the existence of self-trapped states and accounts quantitatively for the positron-annihilation rate in the range of densities and temperatures over which these states are stable. The droplets have a maximum density $2.4 \times 10^{22} \text{ cm}^{-3}$ and are typically 15 to 25 Å in radius.

The positron-lifetime spectrum in helium in the vicinity of the gas-liquid critical point has been observed to possess a number of unusual features.¹ At some time ($\approx 10 \text{ nsec}$) after the introduction of positrons into the gas, the positron annihilation rate is found to increase suddenly to a value corresponding to liquid densities. A qualitative explanation of this behavior was the suggestion² that the increased rate was due to the annihilation of the positron from a localized state confined within a high-density helium cluster, the state being populated after sufficient time had elapsed for the positron to have thermalized. Subsequent measurements³⁻⁵ have confirmed the effect and have established the range of gas densities and temperatures over which the enhanced annihilation rate occurs.

In contrast to this behavior for the positron it is well known that electrons in helium⁶ and positronium in many liquefied gases⁷ may be self-trapped in bubbles. The possibility of positron self-trapping in metals has been studied theoretically⁸ but experimental evidence is inconclusive. Helium appears to be the first system for which positron self-trapping is definitely exhibited. It is, therefore, of interest to understand the nature of positron self-trapping in helium and

to determine those properties which make the self-trapped state stable. In this Letter we present a theory which can account quantitatively for most of the experimental observations on this system.

Initial attempts³ to account for the self-trapped state were based on Atkin's "snowball" model⁹ used in describing the helium density distribution around a fixed ion. This calculation, which treats the positron-helium interaction from a macroscopic point of view, fails to produce a self-trapped state since it does not fully account for the energetics of a positron in a polarizable medium. Provided that the spatial variation of the helium density is small on the scale of the range of the positron-helium interaction, the relevant quantity is the ground-state energy of a positron, $E_0(n)$, in a uniform system of mean density n . Since the net interaction is attractive, $E_0(n)$ is negative and decreases in value with increasing helium density. It is this feature, together with the easy compressibility of the gas near the critical point, which leads to the stability of the self-trapped state.

An approximate thermodynamic potential which describes the fully interacting positron-helium system is

$$\Omega[n, \psi] = \int d^3r f(n(\vec{r}))n(\vec{r}) - \mu(n_0) \int d^3r n(\vec{r}) + \int d^3r \int d^3r' K(\vec{r}, \vec{r}'; [n]) [n(\vec{r}) - n(\vec{r}')]^2 - (\hbar^2/2m) \int d^3r \psi^*(\vec{r}) \nabla^2 \psi(\vec{r}) + \int d^3r E_0(n(\vec{r})) |\psi(\vec{r})|^2. \quad (1)$$

The potential is a functional of the helium density distribution $n(\vec{r})$ and the positron wave function $\psi(\vec{r})$. The first three terms are contributions from the helium alone; the fourth is the positron kinetic energy, and the last is the positron-helium interaction energy. In (1), $f(n)$ is the Helmholtz free energy per particle for a helium density n at a fixed temperature T , and $\mu(n) = \partial(fn)/\partial n$ is the chemical potential. The third term in (1) accounts explicitly for nonuniformities in the helium density. The equilibrium state of the system is determined by those functions $n(\vec{r})$ and $\psi(\vec{r})$ for which Ω attains an absolute minimum.

The interaction kernel $K(\vec{r}, \vec{r}'; [n])$ is unknown in general; however, in the case of small density inhomogeneities it can be related to the density response function $\chi(\vec{q})$ for the uniform system.^{10,11} If, in addition, the variations in density over distances of the order of interparticle separations are small, a density gradient expansion can be used and yields $\frac{1}{2} \int d^3r g(n(\vec{r})) |\nabla n(\vec{r})|^2$ for the third term where $g(n)$ is the q^2 coefficient of a small- q expansion of $\chi^{-1}(\vec{q})$. With these approximations, the variation of Ω with respect to n and ψ leads to the Euler equations

$$|\psi|^2 dE_0/dn = -[\mu(n) - \mu(n_0)] + g(n) \nabla^2 n + \frac{1}{2} g'(n) |\nabla n|^2, \quad (2)$$

$$-(\hbar^2/2m) \nabla^2 \psi + E_0(n) \psi = \epsilon \psi. \quad (3)$$

Rather than solving these equations directly, the thermodynamic potential Ω was evaluated using an explicit trial wave function $\psi_{\text{tr}}(\vec{r})$ and the corresponding helium density obtained from (2) upon neglecting the gradient terms. This procedure gives an upper bound to Ω and the lowest upper bound was obtained by varying parameters in $\psi_{\text{tr}}(\vec{r})$.

Calculations have been performed for ^4He and the required thermodynamic quantities were obtained from an empirical equation of state.¹² In obtaining the gradient correction, the fluctuation-dissipation theorem was used to express $\chi(\vec{q})$ in terms of the dynamical form factor $S(\vec{q}, \omega)$.¹³ By performing a high-temperature expansion and omitting terms involving frequency moments of $S(\vec{q}, \omega)$ greater than the second, the following expression for $g(n)$ is obtained:

$$g(n) = \frac{1}{6} (nkT)^{-1} \left(\frac{\partial P}{\partial n} \right)_T^2 \left[\nu_2 + \frac{\hbar^2}{2kTm_{\text{He}}} \right], \quad (4)$$

where ν_2 is given in terms of the radial distribu-

tion function $g(r)$ by

$$\nu_2 = n \int d^3r r^2 [g(r) - 1]. \quad (5)$$

The validity of (4) is supported by $\hbar^2/2kTm_{\text{He}}$ being typically less than 5% of ν_2 in the temperature range of interest. The expression for $g(r)$ in the limit of low densities, $g(r) = \exp[-\varphi(r)/kT]$ was used in (5) to evaluate ν_2 . Although this approximation yields a poor result for the compressibility, ν_2 was found to be insensitive to the density dependence of $g(r)$ as explicit self-consistent Percus-Yevick calculations at a number of (n_0, T) values above the critical point demonstrated. The helium-helium interaction potential, $\varphi(r)$, was taken to be the effective Lennard-Jones potential¹⁴ which gives classically the correct second virial coefficient, $(\partial P/\partial n)_T$ in (4), however, was determined from the equation of state.¹²

The ground-state energy $E_0(n)$ was calculated using an adaptation of the positron pseudopotential method developed for metals.¹⁵ The positron-helium-atom interaction consists of an attractive polarization contribution behaving as $-\alpha/r^4$ for large separations, where α is the helium-atom polarizability, and a short-ranged electrostatic repulsive term. The polarization term was taken from the work of Reeh¹⁶ while the Hartree term was taken from Kestner *et al.*¹⁷ Since the potential is approximate, the monopole part of the Reeh potential was scaled so that the total potential used in these calculations gave a scattering length equal to the best theoretical estimate ($a_0 = -0.524$ a.u.).¹⁸ $E_0(n)$ was calculated to second order in the positron pseudopotential using Eq. (23) of Ref. 15 with the reciprocal lattice sum replaced by a sum over all \vec{k} space and again taking the temperature-dependent low-density form for the structure factor, $|S|^2$. The result, in meV, is

$$E_0(n) = -E_1 n - E_2 n^2, \quad (6)$$

where $E_1 = 132.4$ and E_2 varies from 14.08 to 3.22 as T increases from 5 to 10 K and n is in units of 10^{22} cm^{-3} .

With this input, Ω was calculated as described above as a function of n_0 and T . The variational wave function,

$$\psi_{\text{tr}}(r) = \left(\frac{3}{4\pi\sigma^3} \right)^{1/2} \exp \left[-\frac{1}{2} \left(\frac{r}{\sigma} \right)^3 \right],$$

gave the lowest values for all single-parameter functions tried, and stable self-trapped states were indeed found. Once the lowest value of Ω

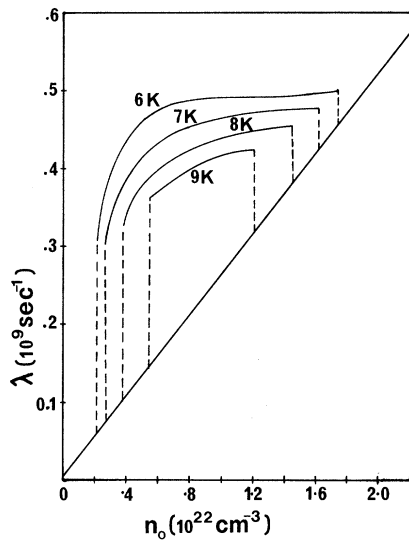


FIG. 1. Calculated positron-annihilation rate, λ , plotted as a function of helium mean density, n_0 , for different values of the temperature. The straight line is the observed (Ref. 5) free-positron-annihilation rate as a function of n_0 .

had been obtained the corresponding wave function and helium density were used to calculate the positron-annihilation rate for the self-trapped state from

$$\lambda_t = \int d^3r |\psi_{tr}(\vec{r})|^2 \lambda_f(n(\vec{r})), \quad (7)$$

where $\lambda_f(n)$ is the observed annihilation rate for the free (unbound) state and mean gas density n . The experimental data⁵ give $\lambda_f(n) = 0.261 \times 10^9 n$ sec^{-1} .

Annihilation rates from (7) are shown as functions of mean helium density for different temperatures in Fig. 1. For a given temperature, self-trapping occurs at some minimum density and the annihilation rate rises sharply to a plateau. If the mean density is increased further there is a maximum density beyond which the droplet becomes unstable and the positron becomes free, with a corresponding drop in annihilation rate back to the free-state value. Observation of the drop in rate at high densities depends somewhat on the value of the rate in the plateau region. Our values are typically 20% higher than the experimental ones and the effect is therefore accentuated. More detailed experimental data in this region is required to determine whether this effect is real.

As the temperature increases, the onset of self-trapping occurs at higher densities and the

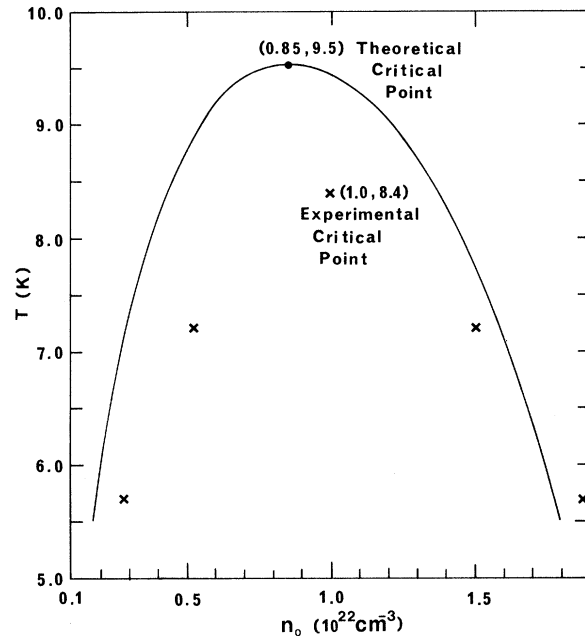


FIG. 2. Phase diagram for droplet formation. The calculated region of droplet stability lies below the full line. Experimental points (Ref. 5) are also shown.

rate in the plateau region has a smaller value. In addition there is a critical temperature above which the self-trapped state is unstable for all densities. The range of stability of the self-trapped state is given well by the model as the phase diagram in Fig. 2 shows. The critical temperature of 9.5 K and the critical density of $0.85 \times 10^{22} \text{ cm}^{-3}$ compare favorably with the experimental values⁵ of 8.4 K and $1.0 \times 10^{22} \text{ cm}^{-3}$, respectively.

The droplet profile is shown in Fig. 3 for different mean densities n_0 at a temperature of 6 K. A general feature is that the droplet size does not grow above 25 Å in radius and contains from 300 to 500 atoms. At low densities the droplet has a sharp interface. However this feature would be smoothed out by an exact treatment of Eqs. (2) and (3) as opposed to the approximate treatment of the density gradient terms and the variational method adopted here. For values of n_0 above the gas-liquid critical density the drops are smoother and our treatment is expected to be reliable. It is to be noted that the maximum total density in the drop is insensitive to mean density and also to temperature.

There is generally good agreement with experiment⁵ although the calculated droplet is slightly

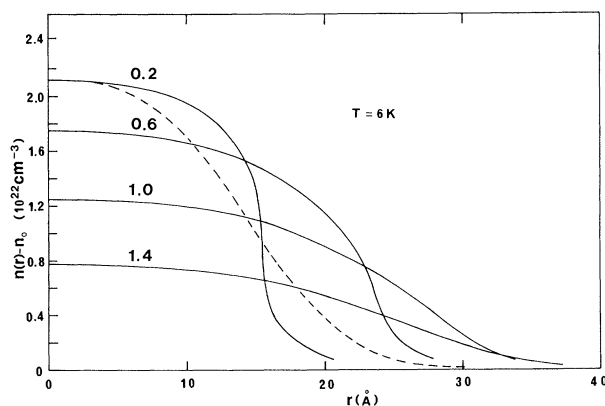


FIG. 3. The excess helium density distribution, $n(r) - n_0$, for the calculated droplets plotted as a function of r for different values of the mean density, n_0 , in units of 10^{22} cm^{-3} at $T = 6 \text{ K}$. The positron wave function, $\psi_{\text{tr}}(r)$, is shown (broken line) for the case $n_0 = 0.2 \times 10^{22} \text{ cm}^{-3}$.

more stable than that observed. In fact, an exact solution of Eqs. (2) and (3) would yield an even more stable droplet. However, it should be pointed out that the calculations have been performed with no adjustable parameters and the results are sensitive to the interaction energy $E_0(n)$; a 10% reduction in its magnitude would lead to a calculated critical point in agreement with experiment. Furthermore, in making contact with experiment we have assumed that the positron thermal energy is much less than its binding energy to the droplet. This cannot be the case when the drop is initially formed and for some time after. Until energies of the order of the binding energy can be dissipated, the positron will not be at thermal energies, the drop will be less stable, more extended in size, and the observed annihilation rate smaller. The features in the vicinity of the discontinuities in the annihilation-rate curve (Fig. 1) may also be modified. Further theoretical work into the kinetics of the droplet formation is required to clarify the situation.

As shown by experiment³ the self-trapped state also occurs below the helium critical point. It may also occur near the critical point of the other rare gases.¹⁹ The conditions for stable self-trapping are not stringent—either a sufficiently strong attractive interaction with an easily compressible medium for droplet formation or a sufficiently strong repulsive interaction for bubble

formation. The conditions for droplet formation are most favorable near a critical point where the compressibility diverges. The theory developed here is to be extended and applied to these other situations.

We are grateful to the authors of Ref. 5 for communicating their results prior to publication.

*Work supported by the National Research Council of Canada.

¹S. J. Tao, J. Bell, and J. H. Green, Proc. Phys. Soc., London **83**, 453 (1964); W. R. Falk and G. Jones, Can. J. Phys. **42**, 1751 (1964).

²L. O. Roellig, in *Positron Annihilation*, edited by A. T. Stewart and L. O. Roellig (Academic, New York, 1967), p. 127.

³K. F. Canter, J. D. McNutt, and L. O. Roellig, Phys. Rev. **12**, 375 (1975).

⁴M. Fishbein and K. F. Canter, Phys. Lett. **55A**, 398 (1976).

⁵P. Hautajarvi, K. Rystölä, P. Tuovinen, A. Vehanen, and P. Jauho, Phys. Rev. Lett. **38**, 842 (1977).

⁶J. L. Levine and T. M. Sanders, Phys. Rev. **154**, 138 (1967).

⁷C. V. Briscoe and A. T. Stewart, in *Positron Annihilation*, edited by A. T. Stewart and L. O. Roellig (Academic, New York, 1967), p. 377.

⁸A. Seeger, Appl. Phys. **7**, 85 (1975); C. H. Hodges and H. Trinkaus, Solid Status Commun. **18**, 857 (1976); C. H. Leung, T. McMullen, and M. J. Stott, J. Phys. F **6**, 1063 (1976).

⁹K. R. Atkins, Phys. Rev. **116**, 1339 (1959).

¹⁰P. Hohenberg and W. Kohn, Phys. Rev. **136**, B864 (1964).

¹¹C. Ebner and W. F. Saam, Phys. Rev. B **12**, 293 (1975).

¹²D. B. Mann, *Thermodynamic Properties of Helium*, U. S. National Bureau of Standards Technical Note No. 154 (U. S. GPO, Washington, D. C., 1962).

¹³P. C. Martin, in *Many-Body Physics*, edited by C. deWitt and R. Balian (Gordon and Breach, New York, 1968).

¹⁴J. O. Hirschfelder, C. F. Curtiss, and R. B. Bird, *Molecular Theory of Gases and Liquids* (Wiley, New York, 1964).

¹⁵P. Kubica and M. J. Stott, J. Phys. F **4**, 1969 (1974).

¹⁶H. Reeh, Z. Naturforsch. **15a**, 377 (1960).

¹⁷N. R. Kestner, J. Jortner, M. H. Cohen, and S. A. Rice, Phys. Rev. **140**, A56 (1965).

¹⁸S. K. Houston and R. J. Drachman, Phys. Rev. A **3**, 1335 (1971).

¹⁹K. F. Canter and L. O. Roellig, Phys. Rev. **12**, 386 (1975).